Nonlinear differential delay equations using the Poincaré section technique

Zhao Hong,[1] Zhang Feizhou,[1] Yan Jie,[1,2] and Wang Yinghai[1,*]
[1]*Department of Physics, Lanzhou University, Lanzhou, Gansu, 730000, China*
[2]*Institute of Theoretical Physics, Academia Sinica, Beijing, China*
(Received 4 October 1995; revised manuscript received 11 July 1996)

This paper shows that the Poincaré section technique is a powerful tool for representing the solutions of differential delay equations (DDEs). The tool enables us to conveniently identify the periodicity of solutions of a DDE. With this tool we illustrated the fine structure, including the Farey tree structure, of the bifurcation diagram with a DDE related to optical bistability. [S1063-651X(96)03411-3]

PACS number(s): 05.40.+j

In the study of the systems described by differential delay equations (DDEs), researchers get much benefit from the application of numerical methods, such as numerical simulation, power spectrum analysis, and Lyapunov analysis [1,2]. These methods enable them to find that a class of DDEs related to optical bistability may display bifurcation (multifurcation) phenomena [2,3], frequency-locked anomaly [4–6], Hopf bifurcation, quasiperiodic motion [7], and chaotic behavior [1–12]. In order to trace the evolution course of the DDE studied, researchers usually draw the evolution curve of a variable, say, x, with time t. However, it is difficult to distinguish, say, a long periodic orbit from a quasiperiodic or chaotic trajectory if one observes the $x(t)-t$ diagram only. It is the purpose of the present paper to apply the well-known Poincaré section technique to the study of DDEs so as to provide an efficient way of representing its solutions. This is to be done by scattering the $x(t)-t$ curve properly. The DDE investigated by us is of the form

$$\tau\frac{dx(t)}{dt}=-x(t)+f(\mu,x(t-1)),$$

with

$$f(\mu,x)=1-\mu x^2, \tag{1}$$

where $x\in R$ and τ,μ are the system parameters (τ is fixed to 0.81 throughout the paper). To get $x(t)$ we integrate (1) numerically by using a fourth-order Adam interpolation. Equation (1) is considered to have some general characteristics of a kind of DDE related to optical bistability [11,12].

Figures 1(a)–1(c) show three solutions of (1) by drawing the $x(t)$-t diagram: a periodic solution with period $T=3.04$ [Fig. 1(a), $\mu=3.0$], a periodic solution with period $T=19.2$ [Fig. 1(b), $\mu=4.385$], and a chaotic solution [Fig. 1(c), $\mu=4.45$]. By observing this kind of figure only, nobody can distinguish a periodic solution from a quasiperiodic or chaotic solution with confidence. In order to apply the Poincaré section technique, one can write a DDE as a functional differential equation

$$\tau\frac{dx(t)}{dt}=\mathrm{Im}[x_t,\mu],\quad x\in C, \tag{2}$$

where $\{C=x_t|x_t\in C_{[-1,0]},x_t(\theta)=x_t(t+\theta),-1\leqslant\theta\leqslant 0, 0\leqslant t\leqslant\infty\}$, $C_{[-1,0]}$ is a linear space whose elements are continuous functions in $(-1,0)$, and Im: $C\mapsto R$ is a functional. In this form, the dynamics can be well viewed as a continuous-time flow from an initial state x_{t_0} in C. The flow can be written as $x_t(\theta)=\Gamma_\theta(t,t_0)x_{t_0}$, where $\Gamma_\theta(t,t_0):C\mapsto R$ is the evolution operator that maps x_{t_0} to $x_t(\theta)$ and $\Gamma_\theta(t,t)$ is defined as unit operator. This defines a function-to-function map on C,

$$x_{i+1}(\theta)=\Gamma_\theta(t_{i+1},t_i)(x_i), \tag{3}$$

where $x_i\equiv x_{t_i}$ and t_i is the measuring time. In the limit case of $\tau=0$, (3) can be written down explicitly. In the selection of $f(\mu,x)=1-\mu x^2$, it is just the one-dimensional logistic map

$$x_{i+1}(\theta)=1-\mu x_i^2(\theta). \tag{4}$$

In general, one has to get (3) numerically. The way to convert the flow to a map is somehow arbitrary. One can obtain t_i's (and x_i's correspondingly) by simply measuring t with a constant interval b, i.e., $t_{i+1}-t_i=b$. This way corresponds to the stroboscopic sampling techniques used by experimentalists [the sample here is a segment of $x(t)$ between t_i-1 and t_i instead of a finite number of points]. Li and Hao [11] also suggested using it to represent the solutions of DDEs. Figures 1(d)–1(f) show the same solutions given in Figs. 1(a)–1(c), respectively, by using this method in the case of $b=1$. One can find that the periodic solutions appear as quasiperiodic solutions. The reason is that T/b is generally not a rational number. Thus this way of converting the flow to a map is not capable of meeting the purpose to identify the periodic quality of the solutions of DDEs.

In fact, the interval of t_i's does not need to be a constant. One can obtain t_i's in the following way. Choose an appropriate constant $x_c\in R$ (we choose $x_c=0$ for the system studied in the present paper); integrate (1) numerically; and switch on a simulation procedure to get t_i as well as x_i in the condition $x_i(0)=x_c$ when the integrated curve shows

*Author to whom correspondence should be addressed.

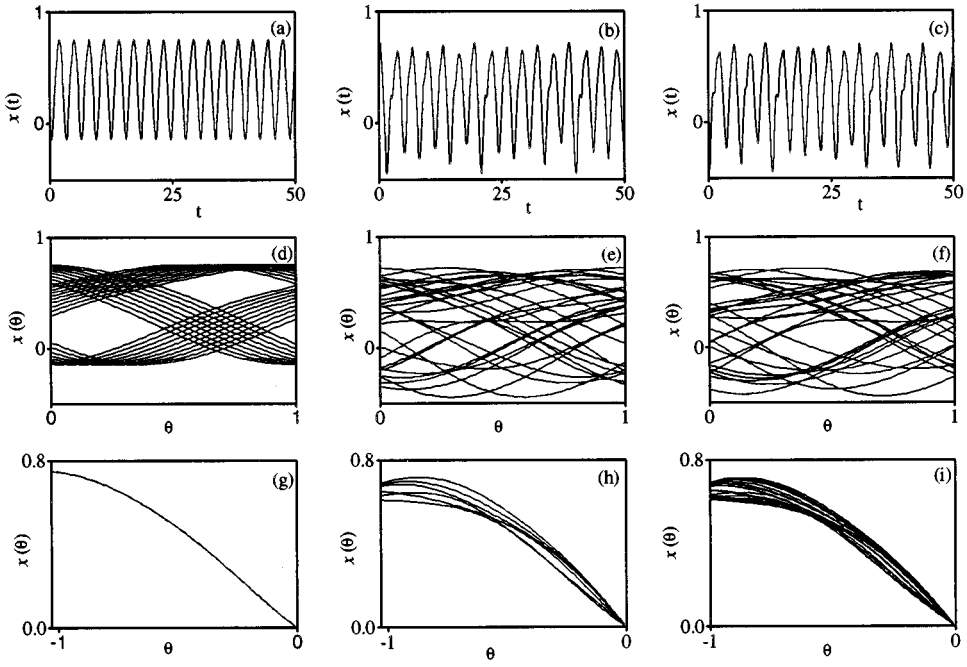

FIG. 1. Geometrical representation of the solutions of (1).

$x(t)>x_c$ and $x(t+h)<x_c$, where h is the length of the integrating step and has been set to 0.001 in the paper. In this way of scattering t, a periodic solution of (1) with period T, $x(t)=x(t+T)$, will correspond to a periodic solution of (3) with period N, $x_i(\theta)=x_{i+N}(\theta)$, uniquely. Figures 1(g)–1(i) show the result by using of this representation. One can find that the periodic solution with period $T=3.04$ appears as one curve [Fig. 1(g)] and the periodic solution with period $T=19.2$ appears as six curves [Fig. 1(h)]. We call them the period-1 solution and the period-6 solution, respectively. Figure 1(i) describes the chaotic solution shown in Fig. 1(c), and the curve in the figure looks irregular. This method of converting a flow to a map is similar to that in the case of finite-dimensional autonomous systems, but the map obtained here is a curve-to-curve map instead of a point-to-point map. Thus we regard the maps obtained in this way as the Poincaré map of DDEs and denote the periodic solution of (1) with the period of the Poincaré map. To illustrate the bifurcation behaviors of the system in a familiar way, we can simply represent the curve x_i by n representative points $x_i(\theta_j)$ $(j=1,2,\ldots,n)$. Then the curve-to-curve mapping appears as a point-to-point mapping in R^n. In practice, one needs only a two-dimensional or a one-dimensional point-to-point representation of the Poincaré map for the usual investigation. For example, one can exhibit the coexistence attractors with a two-dimensional representation in the plane $x_i(d_1)$-$x_i(d_2)$ or investigate the bifurcation behavior of the parameter μ by depicting $x_i(d_1)$, where d_1 and d_2 are constants and $-1<d_i<0$. Figure 2 shows the bifurcation diagrams of several coexisting attractors in the plane $x_i(-0.08)-\mu$. The object originating from a period-N solution is coded by nA. The main branch 1A illustrates an infinite period-doubling process with increasing the parameter μ: a period-1 solution, bifurcates (at $\mu=3.4745$) to a period-2 solution which then bifurcates (at $\mu=4.1065$) to a period-4 solution, which then bifurcates (at $\mu=4.234\,45$) to a period-8 solution. The following bifurcation up to 256 periods takes place at $\mu=4.265\,875$,4.272 915 5,4.274 428 3,4.274 752 8, and 4.274 822 5, respectively, with an accumulation point $\mu=4.274\,841\,496$, beyond which chaos appears. According to the above data, the convergence rate is calculated to be $\delta_1=4.66$. Increasing μ continuously, the chaotic state accumulates to a period-1 solution again through a reversal of period-doubling cascades. We also calculate the convergence rate of the reversal sequence by using the data of the bifurcation points up to 128 periods and get $\delta_2=4.63$. In fact, calculations show that the convergence rates of the period-doubling sequence in some periodicity windows of 1A and in other branches (2A, 3A, and 6A) all seem to agree to the scaling factor. There are abundant the periodicity windows in the chaotic range of 1A. Scanning the range $\mu \in (4.27,4.92)$ with the scale $\delta\mu=5\times10^{-5}$, periodicity windows found are 20, 12, 14, 10, 14, 16, 6, 18, 14, 10, 8, 10, 9,

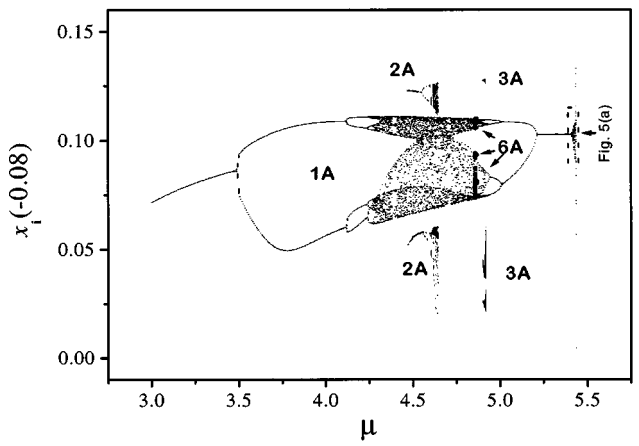

FIG. 2. Bifurcation diagrams of several coexistence attractors of (1). The attractor beginning with a period-N solution is coded by nA.

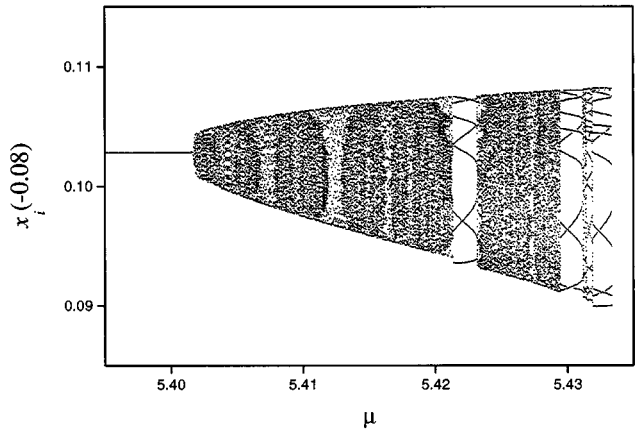

FIG. 3. Enlargement of the broken-line square indicated region of 1A in Fig. 2.

9, 11,10, 8, 10, 16, 18, 10, 14, 12, and 20; here we use the period of the beginning periodic solution in a window to denote the corresponding periodicity window and only periodicity windows less than 20 are listed. Dividing the sequence into two parts at the two 9's, one can see that most numbers on the left-hand side can be found in the symmetrical position on the right-hand side. In fact, it seems that the right-half of 1A is a mirror of the left-hand side of 1A. However, the right-hand side of 1A disappears suddenly with decreasing τ, whereas the left half remains all the way and the periodic wave forms in it appear to be the continuous-time counterparts of the discrete cycles predicted by the one-dimensional model, the logistic map. Figure 3 is an enlargement of the area indicated by a broken-line square in Fig. 2. From this figure one can find that a bifurcation occurs at $\mu=5.401$. The process of the bifurcation in a two-dimensional Poincaré section and the Lyapunov exponents calculations indicates that the bifurcation is a Hopf bifurcation. After the Hopf bifurcation, Fig. 3 indicates that there exists a quasiperiodic solution region embedded with many periodic solutions. In fact, scanning the region with a finer scale of the parameter step, one can find numerous periodic solutions. Scanning the range $\mu\in(5.401,5.435)$ with parameter steps of $\delta\mu=1\times10^{-6}$, we get the following sequence of stable period solutions (only periods less than 80 are listed): 71, 33, 61, 68, 79, 51, 74, 23, 64, 41, 59, 77, 18, 67, 49, 31, 75, 44, 57, 70, 13, 73, 60, 47, 34, 55, 76, 21, 71, 50, 29, 66, 37, 53, 8, 75, 67, 59, 51, 43, 78, 27, 46, 68, 19, 49, 30, 42, 11, 36, 61, 61, 25, 64, and 14. It is found that the sequence is just a part of the well-known ''Farey sequence.'' In the case of the circle map, a periodic orbit is denoted by a rational fraction p/q, where q indicates that there are q points on the circle, i.e., q is the period of the orbit, and p

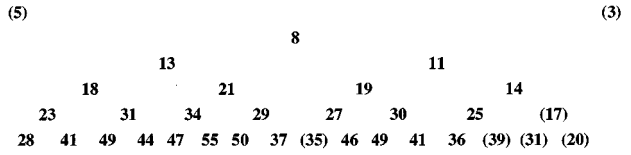

FIG. 4. Farey tree structure of (1).

indicates that each of the q points is visited in p full turns. When the frequency locking occurs, this periodic orbit can be observed within a parameter regime. Between two frequency-locked regimes, described by rational fractions p/q and p'/q', respectively, the most easily observable, i.e., the widest in the parameter space, period would be given by the Farey composition $p/q\oplus p'/q'=(p+p')/(q+q')$. In the example here, we omit the calculation of the full turn number p for simplicity and then the Farey composition turns into $q\oplus q'=(q+q')$. Applying this composition rule to $q=5$ and $q'=3$, one gets 8, which is the widest periodic solution in the parameter space (see Fig. 3). Reapplying the Farey construction to all adjacent pairs, one arrives at a Farey tree, shown in Fig. 4. One can find the numbers in the tree except those with parentheses, which are found in the above stable periodic solution sequence. In fact, we examined all the periodic solutions in the above sequence and found that they obey the Farey composition rule, except for the two adjacent period-61 solutions, which should be one period-61 solution according to the Farey construction. The existence of the stable Farey construction periodic solutions indicates that frequency locking occurs here. The locked frequencies are the two frequencies in tours and the mechanics is similar to that of the circle maps.

In conclusion, the Poincaré section technique is a powerful tool in the study of DDEs. This tool provides us with an efficient method of representing the solutions of DDEs geometrically. With this representation, one can easily identify different periodic solutions, describe the quasiperiodic solutions, demonstrate coexist solutions, and investigate the bifurcation behaviors. We have investigated (1) in detail and shown the fine structure of the bifurcation diagram. We found that besides the period-doubling bifurcation the Hopf bifurcation of periodic solutions may also take place in the systems described by (1). After the Hopf bifurcation threshold, there appears a quasiperiodic regime that is embedded with the Farey sequence of stable periodic solutions. Taking the other forms of $f(\mu,x)$ in Eq. (1), say, $f(\mu,x)=\pi\mu\sin(x-x_0)$ as Ikeda and Matsumoto adopted [2], similar phenomena have been observed.

We acknowledge fruitful discussions with Professor B. L. Hao and Professor Y. Gu. This work is supported by Gansu provincial Natural Science Foundation of China.

[1] J. D. Farmer, Physica D **4**, 366 (1982).
[2] K. Ikeda and K. Matsumoto, Physica D **29**, 223 (1987).
[3] J. Y. Gao, L. M. Narducci, L. S. Schulman, M. Squicciarini, and J. M. Yuan, Phys. Rev. A **28**, 2910 (1983).
[4] F. A. Hopf, D. L. Kaplan, H. M. Gibbs, and R. L. Sheomaker, Phys. Rev. A **25**, 2172 (1982).
[5] K. Ikeda, K. Kondo, and O. Akimoto, Phys. Rev. Lett. **49**, 1467 (1982).

[6] R. Vallée and C. Delise, Phys. Rev. A **34**, 309 (1986).
[7] M. Le Berre, E. Ressayre, and A. Tallet, Opt. Commun. **72**, 123 (1989).
[8] K. Ikeda and O. Akimoto, Phys. Rev. Lett. **48**, 617 (1982).
[9] H. M. Gibbs, F. A. Hopf, D. L. Kaplan, and R. L. Shoemaker, Phys. Rev. Lett. **46**, 474 (1982).
[10] B. Dorizzi, B. Grammaticos, M. Leberre, Y. Pomeau, E. Ressayre, and E. Tallet, Phys. Rev. A **35**, 328 (1987).
[11] J.-N Li and B.-L Hao, Commun. Theor. Phys. **11**, 265 (1989).
[12] J. Losson, M.C. Mackey, and A. Longtin, Chaos **3**, 167 (1993).